J. Biochem. 2010;147(1):109–115 doi:10.1093/jb/mvp154

JB THE JOURNAL OF BIOCHEMISTRY

Crystal structure of peroxiredoxin from *Aeropyrum pernix* K1 complexed with its substrate, hydrogen peroxide*

Received June 10, 2009; accepted September 3, 2009; published online October 9, 2009

Tsutomu Nakamura[1,†,‡], Yuji Kado[2,‡], Takafumi Yamaguchi[2,§], Hiroyoshi Matsumura[2], Kazuhiko Ishikawa[1] and Tsuyoshi Inoue[2]

[1]National Institute of Advanced Industrial Science and Technology, Ikeda, Osaka 563-8577; and [2]Graduate School of Engineering, Osaka University, Suita, Osaka 565-0871, Japan

*The atomic coordinates and structure factors have been deposited in the Protein Data Bank, www.pdb.org (PDB ID codes 3A2V, 3A2W, 3A2X, and 3A5W).

†Tsutomu Nakamura, National Institute of Advanced Industrial Science and Technology, 1-8-31 Midorigaoka, Ikeda, Osaka 563-8577, Japan, Tel: +81 72 751 9272, Fax: +81 72 751 8370, E-mail: nakamura-t@aist.go.jp

‡These two authors equally contributed to this work.
§Present address: Takafumi Yamaguchi, Dia/-Nitric Co. Ltd, Tsurumi, Yokohama, Kanagawa 230-0053, Japan.

Peroxiredoxin (Prx) reduces hydrogen peroxide and alkyl peroxides to water and corresponding alcohols, respectively. The reaction is dependent on a peroxidatic cysteine, whose sulphur atom nucleophilically attacks one of the oxygen atoms of the peroxide substrate. In spite of the many structural studies that have been carried out on this reaction, the tertiary structure of the hydrogen peroxide-bound form of Prx has not been elucidated. In this paper, we report the crystal structure of Prx from *Aeropyrum pernix* K1 in the peroxide-bound form. The conformation of the polypeptide chain is the same as that in the reduced apo-form. The hydrogen peroxide molecule is in close contact with the peroxidatic Cys50 and the neighbouring Thr47 and Arg126 side chain atoms, as well as with the main chain nitrogen atoms of Val49 and Cys50. Bound peroxide was also observed in the mutant C50S, in which the peroxidatic cysteine was replaced by serine. Therefore, the sulphur atom of the peroxidatic cysteine is not essential for peroxide binding, although it enhances the binding affinity. Hydrogen peroxide binds to the protein so that it fills the active site pocket. This study provides insight into the early stage of the Prx reaction.

Keywords: *Aeropyrum pernix* K1/hydrogen peroxide/peroxidatic cysteine/peroxiredoxin/thioredoxin peroxidase.

Abbreviations: ApTPx, thioredoxin peroxidase from *Aeropyrum pernix* K1; C_p, peroxidatic cysteine; Prx, peroxiredoxin.

Peroxiredoxins (Prxs) are thiol-dependent peroxidases that reduce hydrogen peroxide and alkyl peroxides to water and corresponding alcohols, respectively (*1–3*). By removing peroxide species, Prxs function in the cellular defence system against reactive oxygen species that damage biological molecules such as proteins, nucleic acids and lipids (*4*). In addition, Prxs regulate intracellular levels of hydrogen peroxide, which affects signal mediators such as protein tyrosine phosphatase (*5*) and lipid phosphatase PTEN (*6*) through the self-inactivation mechanism (*7*).

There are several oligomeric states of Prxs: monomer, dimer, decamer and dodecamer (*8*). To date, there have been three types of reaction cycle proposed for Prxs. Based on the resolving process of the oxidized forms, Prxs are divided into three classes: typical 2-Cys, atypical 2-Cys and 1-Cys Prxs (*1*, *9*). In spite of these varied reaction mechanisms, Prxs have a highly conserved active site containing a reactive cysteine residue—the peroxidatic cysteine (C_p). The side chain of C_p has a lower pK_a value than that of a free thiol group because of its interaction with a base. The thiolate form attacks the peroxide substrate to generate cysteine sulphenic acid or its derivative (*10*).

Previously, we have reported the tertiary structure of an archaeal Prx, the thioredoxin peroxidase from *Aeropyrum pernix* K1 (ApTPx) and described the structural changes that occur upon oxidation (*11–13*). To date, the tertiary structures of archaeal Prxs have been elucidated for two proteins, ApTPx (the product of ORF APE_2278) (*12*, *14*) and the bacterioferritin comigratory protein Prx from *A. pernix* K1 (the product of ORF APE_2125) (Mizohata *et al.*, unpublished, PDB codes 2CX3 and 2CX4). The overall structure of ApTPx consists of a decameric ring made up of five homodimers. Each monomer structure can be divided into the N-terminal main domain and the C-terminal arm domain. The main domain is conserved in all Prxs and consists of a thioredoxin fold with five α-helices and seven β-strands, whereas the arm domain is unique to ApTPx (*12*). The peroxidatic cysteine, C_p50, is situated at the first turn of α-helix 2 in the main domain. Upon oxidation by hydrogen peroxide, the active site undergoes a conformational change and C_p50 forms a hypervalent sulphur intermediate, a sulphurane derivative, through a covalent linkage between S^{γ} of C_p50 and $N^{\delta 1}$ of the neighbouring His42 side chain (*13*). However, it is not clearly understood how the reaction starts, because of the lack of structural details on the interaction between the substrate hydrogen peroxide and the active site of ApTPx in the reduced state.

To date, there have been no reports on the tertiary structure of Prx complexed with its substrate, hydrogen peroxide. Instead, a recent review on the structure of Prxs discussed peroxide binding to the active site by

Downloaded from http://jb.oxfordjournals.org/ at Islamic Azad University on September 28, 2012

© The Authors 2009. Published by Oxford University Press on behalf of the Japanese Biochemical Society. All rights reserved

analogy to the crystal structure of human PrxV bound with benzoate. In that structure, the two carboxylate oxygens mimic the placement of the two oxygens of a peroxide substrate (*8*, *15*). In this paper, we describe the interaction of Prx with hydrogen peroxide by presenting the crystal structure of ApTPx complexed with the true substrate. Based on the results, we discuss the reaction mechanism at the early stage of the ApTPx reaction.

Materials and methods

Protein purification and crystallization

We used wild-type ApTPx and the ApTPx mutants C50S and C207S. Protein purification was performed as described previously (*11*). The proteins were crystallized using the hanging-drop vapour-diffusion method at 20°C. We used either acetate-containing or acetate-free reservoir conditions. The former consisted of 0.1 M imidazole–HCl, pH 6.5, and 1 M sodium acetate, and the latter consisted of 0.1 M HEPES–NaOH, pH 7.5, and 0.8 M potassium sodium tartrate.

Substrate binding, data collection and processing

Treatment with hydrogen peroxide was performed by soaking the protein crystals in the corresponding reservoir solution supplemented with 22.5% (v/v) glycerol and 1 mM hydrogen peroxide for durations described in the Results section. The crystals were cooled in a nitrogen gas stream (100 K) and subjected to X-ray diffraction measurements with synchrotron radiation in SPring-8 (Harima, Japan). The collected data were integrated and scaled with HKL2000 (*16*). The structural refinement was performed with REFMAC in the ccp4 suite (*17*) or with CNS (*18*).

Results

Binding of hydrogen peroxide to the peroxidatic cysteine

For the ApTPx proteins with intact C_p50, we carried out crystallographic studies with the wild-type and C207S mutant. As described previously (*13*), the C_p side chain is oxidized when crystals are soaked in a solution containing 1 mM hydrogen peroxide for 1 min prior to collection of diffraction data. Indeed, the oxidized species—the hypervalent sulphur form of ApTPx—was reproducibly observed as described previously (*13*). In this study, we reduced the soaking time in order to detect the hydrogen peroxide molecule bound to the active site of ApTPx before the protein was oxidized.

We obtained the peroxide-bound form in C207S mutant as described below, while the wild type did not show the peroxide-bound form clearly as far as tested. However, this does not imply that the wild-type protein cannot exist as the peroxide-bound form (discussed later). In this article, we present the results from the C207S protein for the interaction between hydrogen peroxide and the C_p side chain.

We crystallized the C207S protein and soaked the crystal in a solution containing 1 mM hydrogen peroxide for 20 s (see the Materials and methods section). The crystal structure was refined to 1.65 Å resolution with R_{cryst} and R_{free} values of 19.4 and 22.3%, respectively (Table 1). Figure 1 shows the refined structure

Table 1. Crystallization, data collection and refinement statistics.

PDB code	3A2V	3A2X	3A2W	3A5W
Protein	C207S	C50S	C50S	Wild type
Reservoir[a]	Acetate-containing	Acetate-containing	Acetate-free	Acetate-containing
Data collection				
X-ray source	BL41XU, SPring-8	BL41XU, SPring-8	BL44XU, SPring-8	BL44XU, SPring-8
Space group	P1	P1	P1	P1
Unit cell (Å, °)	$a = 76.21$	$a = 75.93$	$a = 76.26$	$a = 77.61$
	$b = 103.11$	$b = 102.89$	$b = 103.33$	$b = 104.78$
	$c = 104.40$	$c = 104.07$	$c = 104.55$	$c = 106.17$
	$\alpha = 106.02$	$\alpha = 105.90$	$\alpha = 105.72$	$\alpha = 105.91$
	$\beta = 104.91$	$\beta = 105.12$	$\beta = 105.08$	$\beta = 104.92$
	$\gamma = 92.97$	$\gamma = 92.89$	$\gamma = 92.63$	$\gamma = 92.88$
Resolution range (Å)[b]	50.0–1.65 (1.71–1.65)	200–1.90 (1.97–1.90)	50.0–2.30 (2.38–2.30)	50.0–2.20 (2.28–2.20)
R_{merge} (%)[b,c]	4.8 (39.1)	7.1 (36.2)	9.1 (34.8)	9.5 (42.6)
Completeness (%)[b]	94.1 (93.9)	93.8 (91.1)	94.8 (91.1)	94.8 (93.9)
No. of unique reflection[b]	329,538 (32,932)	214,677 (20,800)	122,484 (11,764)	147,958 (14,659)
Redundancy[b]	2.1 (2.1)	1.9 (1.8)	1.8 (1.7)	2.1 (2.0)
$I/\sigma(I)$[b]	10.4 (1.4)	6.7 (1.4)	12.9 (2.2)	9.6 (2.3)
Refinement				
Resolution range (Å)[b]	39.25–1.65 (1.70–1.65)	95.78–1.90 (1.95–1.90)	49.45–2.30 (2.44–2.30)	46.53–2.20 (2.26–2.20)
No. of reflection[b]	312,879 (22,845)	203,394 (14,550)	122,474 (17,548)	140,122 (9,957)
R_{cryst}/R_{free}[b,d,e]	19.4 (28.2)/22.3 (31.8)	19.5 (26.2)/24.3 (31.6)	20.2 (26.7)/24.9 (32.7)	20.9 (25.5)/26.9 (34.6)
RMSD, bond length (Å)	0.014	0.019	0.007	0.033
RMSD, bond angle (°)	1.38	1.751	1.3	2.4
Protein atoms	20,075	19,688	19,725	19,655
Water molecules	908	1459	185	177
Hydrogen peroxide molecules	10	0	3	0
Acetate molecules	0	10	0	0
Ramachandran plot (%)[f]				
Favoured	91.2	91.3	91.5	90.2
Allowed	8.7	8.6	8.5	9.6

[a]See the Materials and methods section. [b]Values in parentheses are for the highest resolution shell. [c]$R_{merge} = \Sigma|I - <I>|/\Sigma\ I$, where I is the intensity of observation I and $<I>$ is the mean intensity of reflection. [d]$R_{cryst} = \Sigma||F_o| - |F_c|/\Sigma|F_o|$, where F_o and F_c are observed and calculated structure factor amplitudes, respectively. [e]R_{free} was calculated using a randomly selected 5% of dataset that was omitted from all stages of refinement. [f]Ramachandran plot was performed for all residues other than Gly and Pro.

Downloaded from http://jb.oxfordjournals.org/ at Islamic Azad University on September 28, 2012

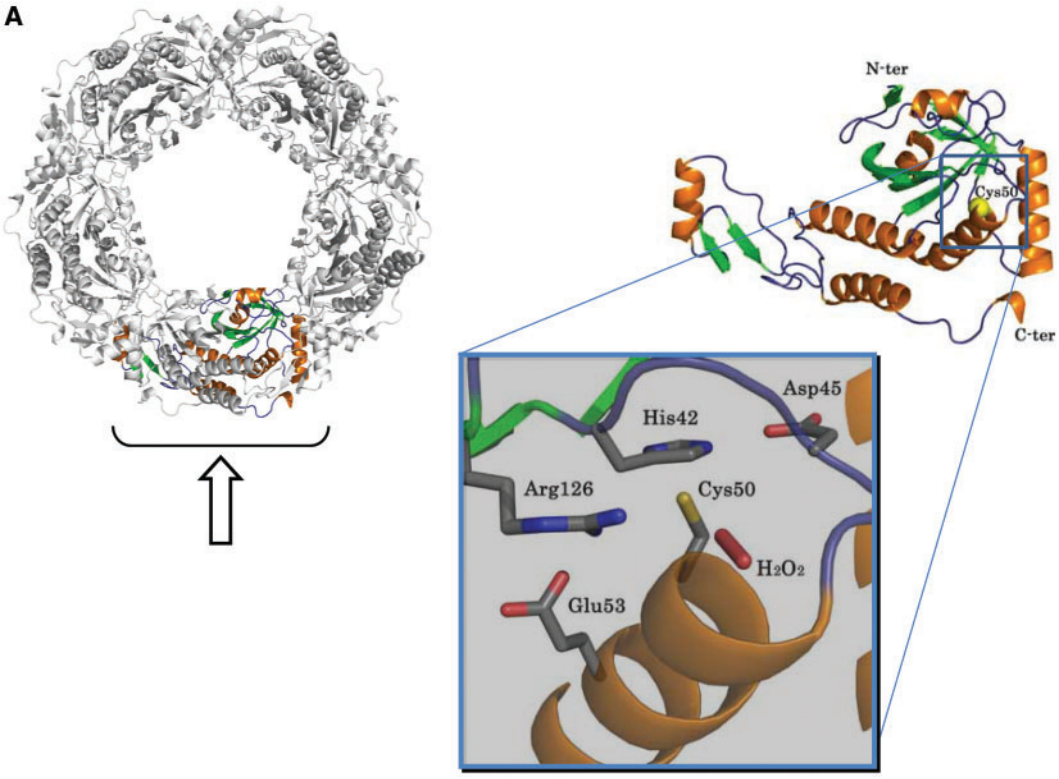

Fig. 1 Crystal structure of peroxide-bound form and reduced form of ApTPx. (A) Whole structure, monomer structure and close-up of the peroxidatic active site of C207S ApTPx (all drawn from the same direction). (B) Structure around active site superimposed onto $2F_0 - F_c$ (blue and green) and $F_0 - F_c$ (magenta) electron density maps contoured at 1.5 σ and 3 σ, respectively. (C) Structure around active site after further refinement assuming a water molecule instead of hydrogen peroxide superimposed onto the electron density maps as shown in (B). (D) Structure around active site of the wild type in the reduced form superimposed onto the electron density maps as shown in (B). Figure drawn with Pymol (*20*) and Molscript (*21*).

of C207S ApTPx. In the crystal structure, the C_p side chain was not oxidized, and the electron density map showed a concentration of electrons in the active site pocket. The electron density coincided well with the hydrogen peroxide molecule (Fig. 1B). When the electron density was assumed to represent a water molecule, a significant positive difference Fourier map was observed (Fig. 1C). The possibility of two water molecules occupying the electron density was excluded, because the distance between the molecules would be too close (1.81 ± 0.20 Å, average ± SD of the 10 subunits). The polypeptide conformation around the active site was the same as that in the reduced form. One of the oxygen atoms of the hydrogen peroxide interacted with C_p50 (S^{γ} and N), Val49 (N), Thr47 (O^{γ}) and Arg126 (N^{η}), and the other interacted with Val49 (N).

Role of the peroxidatic sulphur atom

Structural studies on the ApTPx variant C50S can clarify the interaction of the hydrogen peroxide with the peroxidatic sulphur atom of C_p50. The mutant C50S, in which C_p is replaced by serine, was designed to prevent ApTPx from being oxidized. The C50S protein was crystallized and treated with hydrogen peroxide under the same conditions as those used for C207S. The presence of sodium acetate (see Materials and methods section) resulted in an acetate ion, instead of hydrogen peroxide, binding to the active site (Fig. 2A). The two oxygen atoms of the acetate ion interacted with the neighbouring atoms in the same way as those of hydrogen peroxide bound to the C207S protein. One oxygen atom was in close contact with Ser50 (O^{γ} and N), Val49 (N), Thr47 (O^{γ}) and Arg126 (N^{η}), and the other with Val49 (N). This acetate-bound structure was obtained from the crystals of C50S protein incubated with 1 mM hydrogen peroxide prior to crystallization (data not shown). In C207S, hydrogen peroxide bound to the active site more strongly than the acetate ion, but the acetate ion bound to the C50S protein. This implies that the binding affinity of hydrogen peroxide to the active site is lower in the C50S mutant than in the protein with intact C_p50. Thus, C_p has a significant effect on the binding of hydrogen peroxide.

We searched for other crystallization conditions that did not contain acetate to investigate whether hydrogen peroxide can bind to the active site of C50S ApTPx in the absence of the acetate ion. We obtained crystals of the C50S protein from an acetate-free reservoir (see the Materials and methods section). The C50S crystal grown in the new reservoir was soaked in a solution containing 1 mM hydrogen peroxide for 1 min. The crystal diffracted to 2.3 Å resolution and the structure was refined with R_{cryst} and R_{free} values of 20.2 and 24.9%, respectively (Table 1).

Downloaded from http://jb.oxfordjournals.org/ at Islamic Azad University on September 28, 2012

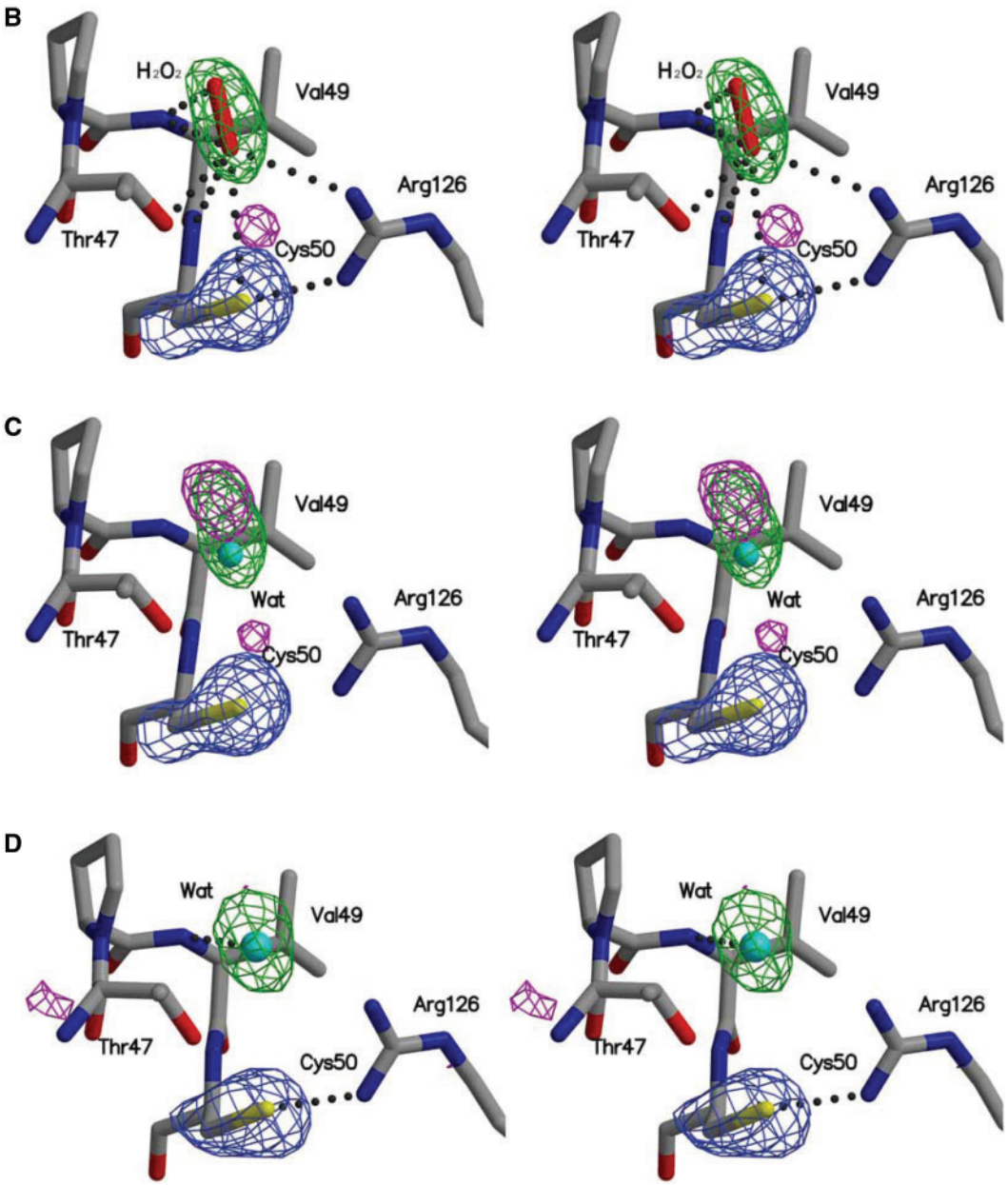

Fig. 1 Continued.

As a result, the crystal structure contained hydrogen peroxide molecules bound to the active site in three subunits among 10 of the overall structure. The interaction of the hydrogen peroxide with the protein atoms was the same as that in the C207S protein, except for interactions involving C_p50 or Ser50. The cryoprotectant glycerol was found at the active sites of the other seven subunits. This result implies that although C_p plays a significant role in binding of hydrogen peroxide, it is not essential.

Binding surface

The active site surface around C_p50 forms a dimple, which is accessible from the interior of the decameric ring of ApTPx (Fig. 3). The surface of the active site is situated near the interacting surface of the homodimer, which is made up of the main domain of one subunit and the arm domain of the other. The surface has a positive electrostatic potential, which is brought by Arg126 side chain. In the peroxide-bound form, the hydrogen peroxide molecule comes in contact with the positive surface and fills in the dimple via the interactions described above. The arginyl side chain changes its configuration along with the reaction coordinate (discussed later). As a result of the conformational change, Arg126 side chain turns to the interior of the molecule and the positive surface potential is neutralized (pre-oxidation form, discussed later).

Discussion

We obtained the peroxide-bound form by in-crystal oxidation of the C207S protein (Fig. 1).

Downloaded from http://jb.oxfordjournals.org/ at Islamic Azad University on September 28, 2012

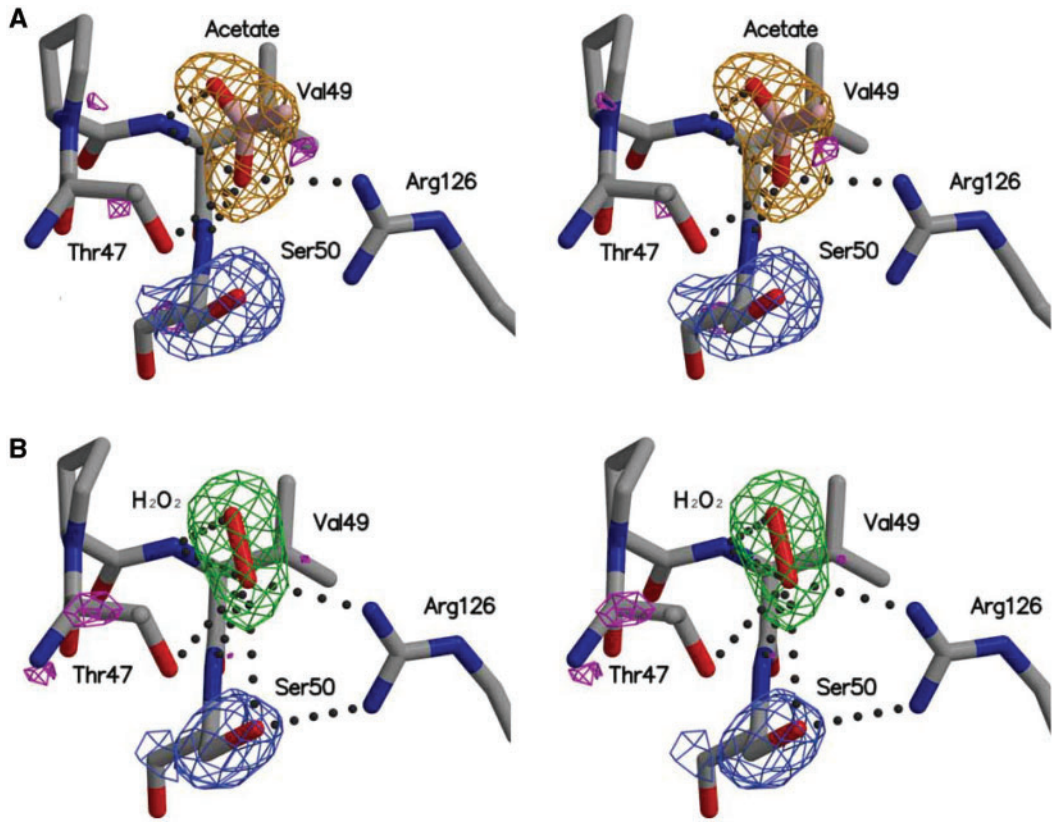

Fig. 2 Crystal structure of C50S mutant treated with hydrogen peroxide. (A) Structure around active site from C50S crystal grown in acetate-containing reservoir followed by soaking in 1 mM hydrogen peroxide for 1 min. Structure is superimposed onto $2F_0 - F_c$ (blue and orange) and $F_0 - F_c$ (magenta) electron density maps contoured at 1.5 σ and 3 σ, respectively. (B) Structure of C50S crystal grown in acetate-free reservoir followed by soaking in 1 mM hydrogen peroxide for 1 min. Structure around active site is superimposed onto $2F_0 - F_c$ (blue and green) and $F_0 - F_c$ (magenta) electron density maps contoured at 1.5 σ and 3 σ, respectively. Figure drawn with Molscript (*21*).

However, we did not obtain the peroxide-bound form with the wild-type crystals. The structure from the wild-type crystals with sufficient resolution was either of the three structures, the hypervalent intermediate, the reduced form (Fig. 1D) and the mixture of the multi conformers of His42 and Arg126 side chains (the conformational change is described later). This does not necessarily imply that the wild-type protein cannot exist as the peroxide-bound form. The reason why we did not detect the peroxide-bound form of the wild type would be because the experimental conditions such as size of the crystal were not controlled precisely. Rather, it is reasonable that the wild-type protein undergoes the peroxide-bound form with certain conditions, since the residues involved in the peroxide binding, as well as other residues, are sterically conserved between the wild-type (reduced form) and C207S mutant. The RMSD value of Thr47, Val49, Cys50 and Arg126 between the wild-type (reduced form) and C207S mutant was 0.474 Å, and that of all non-hydrogen atoms was 0.460 Å.

We have previously reported that the conformation around the active site of ApTPx changes during the interaction with hydrogen peroxide (*13*). In the reduced form, C_p50 interacts with Arg126, which is conserved in all Prxs (illustrated in Fig. 4). With the conformational change, Arg126 swings away from the C_p side chain, and His42 moves near to it. As a result, ApTPx assumes its pre-oxidation form in which the C_p side chain has not been oxidized, while the conformation around the active site is converted from the reduced form. This adopts the configuration of the oxidized species, the hypervalent sulphur form, which is a sulphenic acid derivative of C_p. In this study, we observed the peroxide-bound form of ApTPx, in which the peptide conformation is retained in its reduced form. Therefore, the peroxide binding does not occur after the conformational change of His42 and Arg126 (Fig. 4, pathway 2), nor does it coincide with a conformational change consistent with an induced-fit model. Rather, hydrogen peroxide binds to the reduced form of ApTPx prior to the conformational change (Fig. 4, pathway 1), which is followed by a further oxidation process. It is likely that the positive surface of the active site dimple before the conformational change enhances the binding of hydrogen peroxide.

The pre-oxidation form has been observed at pH 4.8, and the hypervalent sulphur form has been observed at both pH 4.8 and 6.5 (*13*). In this study, however, we did not observe the pre-oxidation form in the crystals grown at pH 6.5, in spite of many trials with various peroxide concentrations and soaking durations. It is likely that the pre-oxidation form is

Downloaded from http://jb.oxfordjournals.org/ at Islamic Azad University on September 28, 2012

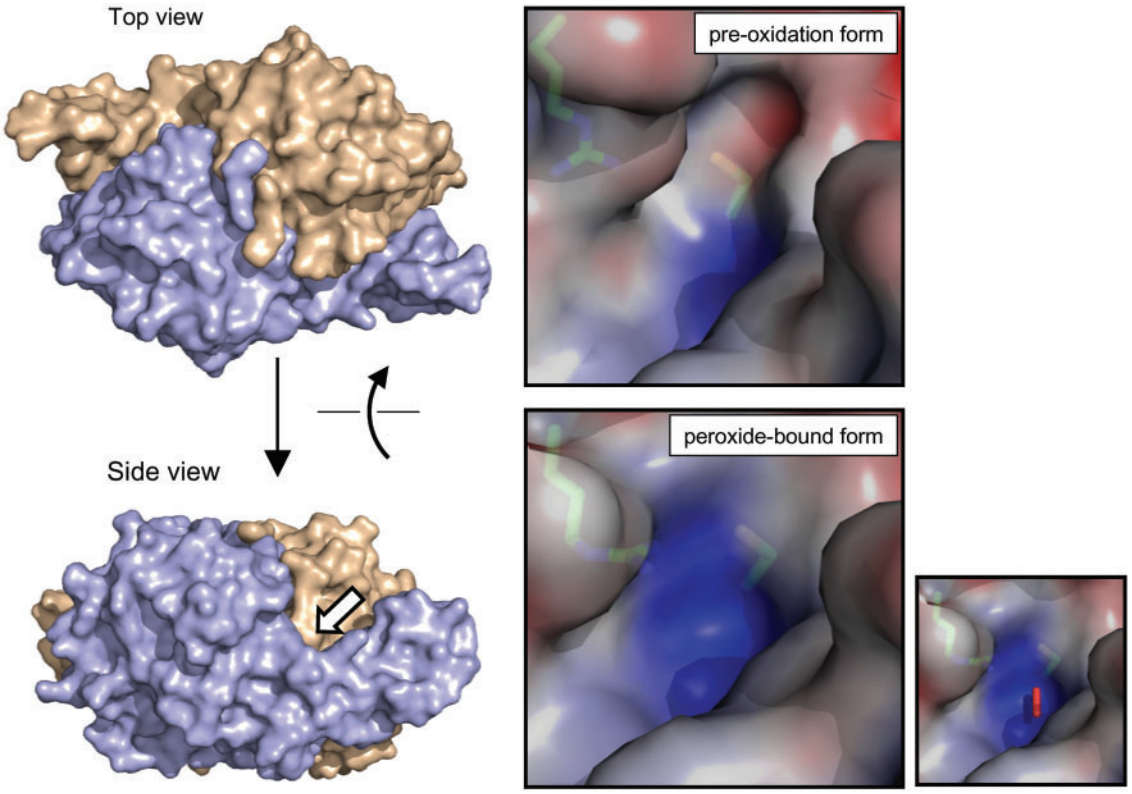

Fig. 3 Surface of ApTPx active site. Molecular surface of C207S homodimer (indicated by an arrow in Fig. 1A). Side view is drawn from the same direction as that in Fig. 1A. Close-ups peroxide-bound form and pre-oxidation form are shown on right. Blue and red indicate positive and negative electrostatic potential, respectively. Hydrogen peroxide molecule on the surface of peroxide-bound form is shown in right. In the pre-oxidation form, clear electron density for hydrogen peroxide was not observed, making it difficult to determine the coordinate of the hydrogen peroxide molecule. Hydrogen peroxide and side chains of C_p50 and Arg126 are shown using stick models. Figure drawn with PyMol (*20*).

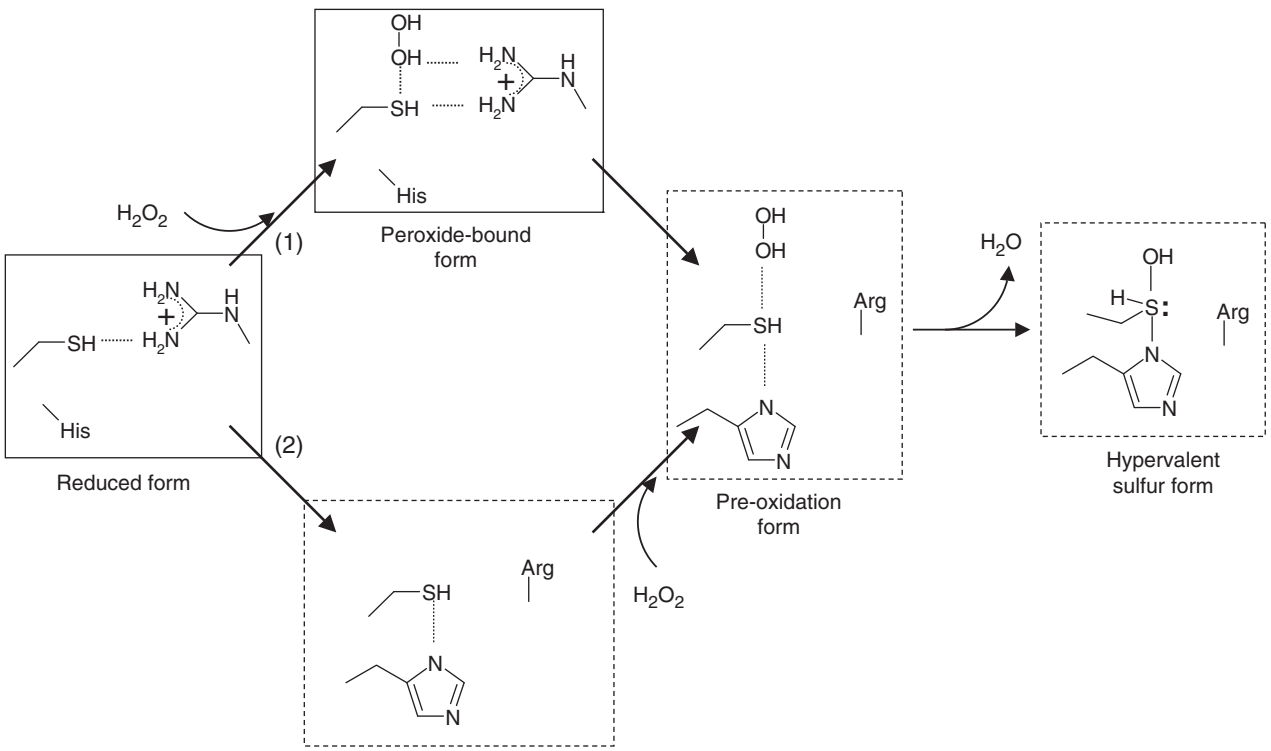

Fig. 4 Proposed reaction scheme of ApTPx. C_p50, His42, Arg126 and hydrogen peroxide are illustrated in the scheme. Solid and dashed boxes show the species before and after conformational change, respectively (see the text). Amino acids in the three-letter code do not interact with other residues shown in the figure. Hydrogen peroxide binds to the active site before and after the conformational change in pathways 1 and 2, respectively.

Downloaded from http://jb.oxfordjournals.org/ at Islamic Azad University on September 28, 2012

trapped only in acidic conditions. If a peroxide molecule situates near C_p in the thiolate form rather than the thiol form, it will be readily attacked by the thiolate to form an oxidized species of C_p, because thiolates are much stronger nucleophiles than are thiol groups. This would explain why the pre-oxidation form was observed in acidic conditions (pH 4.8) but not in neutral conditions (pH 6.5). This is consistent with the pK_a value of C_p estimated for a bacterial Prx AhpC (5.94 ± 0.10) (*19*).

The peroxide-bound form was observed both in C207S and C50S variants of ApTPx (Figs 1 and 2). However, the binding affinity of hydrogen peroxide differed between the proteins with and without intact C_p50. The bound hydrogen peroxide was detected in the C207S crystals grown in the presence of 1 M sodium acetate. Under the same conditions, the C50S protein bound an acetate ion instead of hydrogen peroxide at the active site. This implies that the side chain of C_p promotes the selectivity for hydrogen peroxide binding at the active site, although C_p is not essential for binding.

This is the first report of the tertiary structure of Prx bound with hydrogen peroxide while the peroxidatic cysteine is not oxidized. This study increases our understanding of the very early stages of the Prx reaction.

Acknowledgements

The authors thank Ms. C. Kageyama and Ms. M. Nakatsuka for technical assistance with protein purification and crystallization. The X-ray diffraction studies were carried out at the Japan Synchrotron Radiation Research Institute.

Funding

Grant-in-Aid for Scientific Research (21510237) from Japan Society for the Promotion of Sciences (JSPS).

Conflict of interest

None declared.

References

1. Wood, Z.A., Schroder, E., Robin Harris, J., and Poole, L.B. (2003) Structure, mechanism and regulation of peroxiredoxins. *Trends Biochem. Sci.* **28**, 32–40
2. Hofmann, B., Hecht, H.J., and Flohe, L. (2002) Peroxiredoxins. *Biol. Chem.* **383**, 347–364
3. Rhee, S.G., Kang, S.W., Chang, T.S., Jeong, W., and Kim, K. (2001) Peroxiredoxin, a novel family of peroxidases. *IUBMB Life* **52**, 35–41
4. Halliwell, B. and Gutteridge, J.M. (1984) Oxygen toxicity, oxygen radicals, transition metals and disease. *Biochem. J.* **219**, 1–14
5. Denu, J.M. and Tanner, K.G. (1998) Specific and reversible inactivation of protein tyrosine phosphatases by hydrogen peroxide: evidence for a sulfenic acid intermediate and implications for redox regulation. *Biochemistry* **37**, 5633–5642
6. Lee, S.R., Yang, K.S., Kwon, J., Lee, C., Jeong, W., and Rhee, S.G. (2002) Reversible inactivation of the tumor suppressor PTEN by H_2O_2. *J. Biol. Chem.* **277**, 20336–20342
7. Rhee, S.G., Kang, S.W., Jeong, W., Chang, T.S., Yang, K.S., and Woo, H.A. (2005) Intracellular messenger function of hydrogen peroxide and its regulation by peroxiredoxins. *Curr. Opin. Cell Biol.* **17**, 183–189
8. Karplus, P.A. and Hall, A. (2007) Structural survey of the peroxiredoxins: structures and functions in *Peroxiredoxin Systems* (Flohe L. and Harris J.R., eds.) Vol. 44, pp. 41–60, Springer, New York
9. Chae, H.Z., Robison, K., Poole, L.B., Church, G., Storz, G., and Rhee, S.G. (1994) Cloning and sequencing of thiol-specific antioxidant from mammalian brain: alkyl hydroperoxide reductase and thiol-specific antioxidant define a large family of antioxidant enzymes. *Proc. Natl Acad. Sci. USA* **91**, 7017–7021
10. Poole, L.B. (2007) The catalytic mechanism of peroxiredoxins in *Peroxiredoxin Systems* (Flohe L. and Harris J.R., eds.) Vol. 44, pp. 61–81, Springer, New York
11. Nakamura, T., Matsumura, H., Inoue, T., Kai, Y., Uegaki, K., Hagihara, Y., Ataka, M., and Ishikawa, K. (2005) Crystallization and preliminary X-ray diffraction analysis of thioredoxin peroxidase from the aerobic hyperthermophilic archaeon *Aeropyrum pernix* K1. *Acta Crystallogr. Sect. F Struct. Biol. Cryst. Commun.* **61**, 323–325
12. Nakamura, T., Yamamoto, T., Inoue, T., Matsumura, H., Kobayashi, A., Hagihara, Y., Uegaki, K., Ataka, M., Kai, Y., and Ishikawa, K. (2006) Crystal structure of thioredoxin peroxidase from aerobic hyperthermophilic archaeon *Aeropyrum pernix* K1. *Proteins* **62**, 822–826
13. Nakamura, T., Yamamoto, T., Abe, M., Matsumura, H., Hagihara, Y., Goto, T., Yamaguchi, T., and Inoue, T. (2008) Oxidation of archaeal peroxiredoxin involves a hypervalent sulfur intermediate. *Proc. Natl Acad. Sci. USA* **105**, 6238–6242
14. Mizohata, E., Sakai, H., Fusatomi, E., Terada, T., Murayama, K., Shirouzu, M., and Yokoyama, S. (2005) Crystal structure of an archaeal peroxiredoxin from the aerobic hyperthermophilic crenarchaeon *Aeropyrum pernix* K1. *J. Mol. Biol.* **354**, 317–329
15. Declercq, J.P., Evrard, C., Clippe, A., Stricht, D.V., Bernard, A., and Knoops, B. (2001) Crystal structure of human peroxiredoxin 5, a novel type of mammalian peroxiredoxin at 1.5 Å resolution. *J. Mol. Biol.* **311**, 751–759
16. Otwinowski, Z. and Minor, W. (1997) Processing of X-ray diffraction data collected in oscillation mode. *Methods Enzymol.* **276**, 307–326
17. Collaborative Computational Project, N. (1994) The CCP4 suite: programs for protein crystallography. *Acta Crystallogr. D Biol. Crystallogr.* **50**, 760–763
18. Brunger, A.T., Adams, P.D., Clore, G.M., DeLano, W.L., Gros, P., Grosse-Kunstleve, R.W., Jiang, J.S., Kuszewski, J., Nilges, M., Pannu, N.S., Read, R.J., Rice, L.M., Simonson, T., and Warren, G.L. (1998) Crystallography and NMR system: a new software suite for macromolecular structure determination. *Acta Crystallogr. D Biol. Crystallogr.* **54**, 905–921
19. Nelson, K.J., Parsonage, D., Hall, A., Karplus, P.A., and Poole, L.B. (2008) Cysteine pKa values for the bacterial peroxiredoxin AhpC. *Biochemistry* **47**, 12860–12868
20. DeLano, W.L. (2002) *The PyMol Molecular Graphics System*. DeLano Scientific, Palo Alto, CA, USA
21. Kraulis, P.J. (1991) Molscript—a program to produce both detailed and schematic plots of protein structures. *J. Appl. Cryst.* **24**, 946–950

Downloaded from http://jb.oxfordjournals.org/ at Islamic Azad University on September 28, 2012